



ENGINEERING PHYSICS AND MATHEMATICS

# 2-Amino-3-methyl-3-(4-nitrophenyl)-5-(phenylthio)-3H-pyrrole-4-carbonitrile as effective corrosion inhibitor for mild steel in 1M HCl: Thermodynamical, electrochemical, surface and theoretical calculation



Chandrabhan Verma, M.A. Quraishi \*

Department of Chemistry, Indian Institute of Technology, Banaras Hindu University, Varanasi 221005, India

Received 23 July 2015; revised 3 October 2015; accepted 16 November 2015

Available online 9 February 2016

## KEYWORDS

Mild steel;  
Mixed type;  
EIS;  
SEM/AFM;  
Monte Carlo simulations

**Abstract** Present work describes the corrosion inhibition efficiency of 2-amino-3-methyl-3-(4-nitrophenyl)-5-(phenylthio)-3H-pyrrole-4-carbonitrile (INH) on mild steel in 1M HCl using weight loss, electrochemical, surface and molecular dynamics simulation methods. The weight loss results show that inhibition efficiency increasing with increasing INH concentration and maximum value was obtained at 50 mg/L concentration. Adsorption of the INH on mild steel surface obeys the Langmuir adsorption isotherm. Potentiodynamic polarization study suggests that investigated INH acts as mixed type inhibitor. EIS study indicates that the INH forms a protective surface film at metal/electrolyte interface. Both SEM and AFM studies show that surface smoothness increases due to formation of protective surface film by INH. The Monte Carlo simulation study suggests that INH has strong tendency to adsorb on mild steel surface in 1M HCl. The weight loss, electrochemical, surface and molecular dynamics calculations are in good agreement.

© 2016 Faculty of Engineering, Ain Shams University. Production and hosting by Elsevier B.V. This is an open access article under the CC BY-NC-ND license (<http://creativecommons.org/licenses/by-nc-nd/4.0/>).

## 1. Introduction

Mild steel is one of the most important iron containing alloys used in different applications due to its excellent structural and mechanical strength [1]. However, due to its thermodynamical instability especially in aggressive acid solution it is very prone to corrosion [2]. The hydrochloric and sulfuric acids are two most commonly used acids in the industrial pickling of iron and its alloys to remove unwanted scales and rusts [3]. The poor corrosion resistance of mild steel in acidic solution needs

\* Corresponding author. Tel.: +91 9307025126; fax: +91 542 2368428.

E-mail addresses: [maquraishi@rediffmail.com](mailto:maquraishi@rediffmail.com), [maquraishi.apc@itbhu.ac.in](mailto:maquraishi.apc@itbhu.ac.in) (M.A. Quraishi).

Peer review under responsibility of Ain Shams University.



Production and hosting by Elsevier

utilization of corrosion inhibitors during such processes. Organic compounds containing heteroatoms (N, O, S, and P), heterocyclic rings, polar functional groups and extensive conjugation attract much attention as they inhibit metal corrosion by adsorbing on its surface via several adsorption centers [4]. Moreover, the adsorption on organic inhibitor on metal surface in acid solution depends upon several factors such as electronic structure of inhibitor molecule, steric factors, presence of functional groups (such as  $-\text{OH}$ ,  $\text{NH}_2$ ,  $-\text{NO}_2$ ,  $-\text{CO}$ ,  $-\text{CN}$ ,  $-\text{C}=\text{N}-$ ,  $-\text{N}=\text{N}-$ ), nature of substituents present in the inhibitors, aromaticity, presence of conjugation, molecular weight, solution temperature and electrochemical potential at metal/electrolyte interfaces [5]. The literature survey reveals that inhibitors containing S (sulfur) and N (nitrogen) are useful in sulfuric and hydrochloric acid, respectively, whereas, inhibitor containing both N and S generally gives superior inhibition performance as compared to inhibitor containing only N or S [6]. Present study was undertaken to investigate the corrosion inhibition property of 2-amino-3-methyl-3-(4-nitrophenyl)-5-(phenylthio)-3H-pyrrole-4-carbonitrile (INH) on mild steel surface in 1M HCl. The investigated inhibitor shows high inhibition efficiency due to presence of several polar functional groups ( $-\text{NH}_2$ ,  $-\text{CN}$ ,  $-\text{NO}_2$ ) which increases the solubility as well as inhibition efficiency. Moreover, the  $-\text{NH}_2$  group can easily protonate and form quaternary type of salt and enhance solubility of INH in acid solution. The study was performed using weight loss, potentiodynamic polarization, electrochemical impedance spectroscopy (EIS), scanning electron microscopy (SEM), atomic force microscopy (AFM) and molecular dynamics simulation techniques. In the present study, we intended to find out some suitable molecular dynamic (MD) parameters such as total energy, adsorption energy, rigid adsorption energy, and deformation energy to describe the experimental inhibition efficiency of studied INH.

## 2. Experimental

### 2.1. Inhibitor synthesis

The INH used in the present study was synthesized by one step multi component coupling reaction of p-nitro acetophenone (1 mmol), malononitrile (2 mmol) and thiophenol (2 mmol) in the presence of triethyl amine as catalyst and water as solvent as described earlier [7] (Fig. 1). The characterization data of the synthesized compounds are as follows: INH 2-amino-3-methyl-3-(4-nitrophenyl)-5-(phenylthio)-3H-pyrrole-4-carbonitrile: MP: 173–173 °C, IR (KBr,  $\text{cm}^{-1}$ ): 3478, 3428, 3358, 3256, 3100, 2858, 2218, 1680, 1662, 1598, 1542, 1187, 1024, 710;  $^1\text{H}$  NMR (300 MHz, DMSO,  $\delta$ , ppm,  $\text{Me}_4\text{Si}$ ): 1.63, 6.98, 7.32, 7.56, 7.89–8.13.

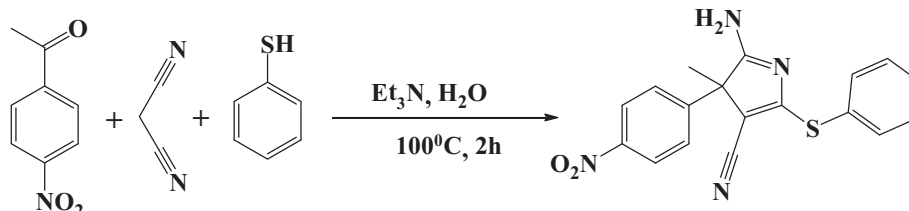


Figure 1 Synthetic scheme for investigated INH.

### 2.2. Preparation of electrodes and test solution

The mild steel specimens have chemical composition: (wt%): C = 0.076, Mn = 0.192, P = 0.012, Si = 0.026, Cr = 0.050, Al = 0.023, and remainder Fe was employed for all weight loss and electrochemical measurements. The mild steel specimens having dimension  $2.5 \times 2 \times 0.025$  cm were used for all weight loss experiments, whereas, mild steel having size  $8 \times 1 \times 0.025$  cm with exposed area  $1 \text{ cm}^2$  was used for all electrochemical measurements. Before performing the experiments, the mild steel surface was successively cleaned with SiC emery papers of different grades (600, 800, 1000 and 1200), washed with double distilled water, degreased with acetone and finally dried under hot air blower. The test solution (1M HCl) was prepared by dilution of analytical grade HCl (MERCK, 37%) in double distilled water. The stock solution of inhibitor was prepared in 1M HCl containing 2% of acetone.

### 2.3. Weight loss experiments

The weight loss experiments were performed on rectangular mild steel specimens in the absence and presence of different concentration of the INH. The volume of solution was 100 ml and immersion time was 3 h. After completion of the immersion time the specimens were taken out, washed with double distilled water, degreased with acetone, ultrasonically cleaned with ethanol, dried and finally weighted accurately. All weight loss experiments were triply performed and mean value was reported to insure the reproducibility. Percentage inhibition efficiency ( $\eta\%$ ) was calculated using the following equation [8]:

$$\eta\% = \frac{w_0 - w_i}{w_0} \times 100 \quad (1)$$

where  $w_0$  and  $w_i$  are the values of weight loss of mild steel in the absence and presence of INH, respectively. The corrosion rate ( $C_R$ ) for mild steel corrosion was calculated using the following equation:

$$C_R (\text{mg cm}^{-2} \text{ h}^{-1}) = \frac{87.6w}{AtD} \quad (2)$$

where  $w$  is the weight loss of mild steel (mg),  $A$  the area of the working electrode ( $\text{cm}^2$ ),  $T$  is the exposure time ( $h$ ) and  $D$  the density of working electrode ( $7.85 \text{ g cm}^{-3}$ ).

### 2.4. Electrochemical experiments

The Potentiostat/Galvanostat (Model G-300), with EIS software Gamry Instruments Inc., USA, containing three electrode electrolytic cell which consists of a pure platinum foil

with exposed area  $1 \text{ cm}^2$  as counter electrode, saturated calomel as reference electrode and mild steel with exposed area  $1 \text{ cm}^2$  as working electrode was employed to carry out all electrochemical experiments. The all electrochemical data were analyzed by Echem Analyst 5.0 software package installed in the computer. Before performing the electrochemical measurements, the mild steel specimens were immersed in 1M HCl for 30 min to stabilize steady state potential. The potentials of working electrode were measured vs. a potential of saturated calomel electrode (SCE).

The potentiodynamic polarization studied was performed by automatically changing the working electrode potentials from  $-0.25$  to  $+0.25$  V vs corrosion potential ( $E_{\text{corr}}$ ) at a scan rate of  $1.0 \text{ mV s}^{-1}$ . The linear segments of Tafel slopes were extrapolated to obtain corrosion current densities ( $i_{\text{corr}}$ ), from which inhibition efficiency was calculated using the following formula [8]:

$$\eta\% = \frac{i_{\text{corr}}^0 - i_{\text{corr}}^i}{i_{\text{corr}}^0} \times 100 \quad (3)$$

where  $i_{\text{corr}}^0$  and  $i_{\text{corr}}^i$  are the corrosion current densities in the absence and presence of INH, respectively.

The electrochemical impedance spectroscopy (EIS) experiments were carried out in between highest frequency limit of 100 kHz and lowest frequency limit of 0.01 Hz at open circuit potential with amplitude of 10 mV using AC signal. Charge transfer resistances were calculated from diameter of the Nyquist curves. The  $\eta\%$  was calculated using the following relation [8]:

$$\eta\% = \frac{R_{\text{ct}}^i - R_{\text{ct}}^0}{R_{\text{ct}}^i} \times 100 \quad (4)$$

where  $R_{\text{ct}}^0$  and  $R_{\text{ct}}^i$  are the charge transfer resistance in the absence and presence of INH, respectively.

## 2.5. SEM

SEM studied was performed on the mild steel specimens after 3 h exposure time in 1M HCl in the absence and presence of optimum concentration of INH using SEM model Ziess Evo 50 XVP instrument with an accelerating voltage of 50 Kv at  $500\times$  magnification.

## 2.6. Atomic force microscopy

The surface morphology of mild steel was investigated using atomic force microscopy after 3 h immersion time at 308 K. The measurements were performed using a NT-MDT multi-mode AFM, Russia, controlled by Solver scanning probe microscope controller. The single beam cantilever having resonance frequency in the range of 240–255 kHz in Semi-contact mode with corresponding spring constant of  $11.5 \text{ N m}^{-1}$  with NOVA programme was used for image interpretation. The scanning area in the images was  $5 \mu\text{m} \times 5 \mu\text{m}$ .

## 2.7. Molecular dynamics simulation measurements

The Monte Carlo simulation was carried out using Adsorption Locator module in Materials Studio 7.0 commercial software licensed from Accelrys Inc., USA. The Monte Carlo (MC)

search was adopted to compute the low configuration adsorption energy of the interactions of the 2-amino-3-methyl-3-(4-nitrophenyl)-5-(phenylthio)-3H-pyrrole-4-carbonitrile on clean iron surface. For the whole simulation procedure, the Universal Force Field (UFF) was used to optimize the structures of all components of the system of interest. The simulation was carried out with Fe (110) crystal with a slab of 5 Å in depth with periodic boundary conditions in order to simulate a representative part of an interface devoid of any arbitrary boundary effects. The Fe (110) plane was next enlarged to a  $(8 \times 8)$  super cell to provide a large surface for the interaction of the inhibitors. After that, a vacuum slab with 30 Å thickness was built above the Fe (110) plane [9].

## 3. Result and discussions

### 3.1. Weight loss measurements

#### 3.1.1. Effect of INH concentration

The variation of inhibition efficiency with INH concentration is shown in Fig. 2a and various weight loss parameters such as corrosion rate ( $C_R$ ), surface coverage ( $\theta$ ) and corresponding inhibition efficiency ( $\eta\%$ ) are given in Table 1. From the results depicted in Table 1 it is observed that the  $\eta\%$  increases with increasing INH concentration. The maximum value of  $\eta$

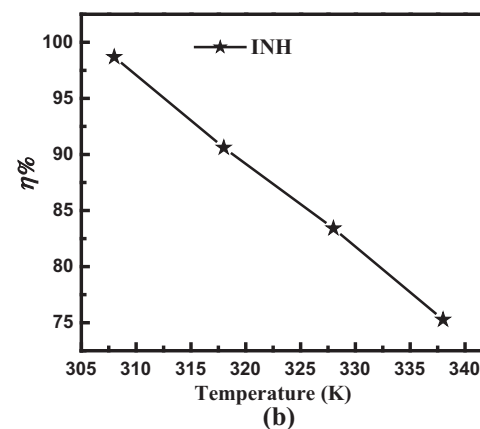
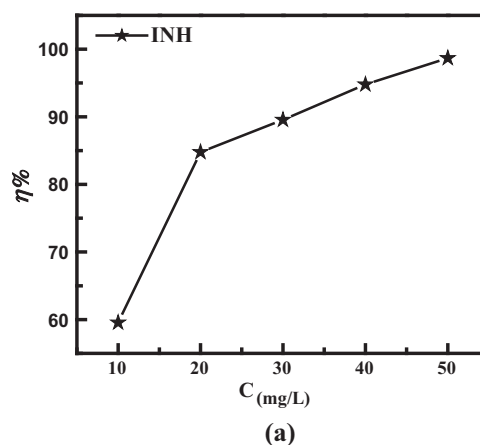


**Figure 2** (a) Variation of inhibition efficiency with INH concentration. (b) Variation of inhibition efficiency with temperature.

**Table 1** The weight loss parameters obtained for mild steel in 1M HCl containing different concentrations of INH.

Inhibitor	Conc (mg/L)	$C_R$ (mg cm <sup>-2</sup> h <sup>-1</sup> )	$\theta$	$\eta\%$
Blank	–	7.66	–	–
INH	10	3.10	0.5953	59.53
	20	1.16	0.8485	84.85
	30	0.80	0.8955	89.55
	40	0.40	0.9477	94.77
	50	0.10	0.9869	98.69

% was obtained at 50 mg/L concentration. Further increase in INH concentration does not cause any significant change in the inhibition performance suggesting that 50 mg/L is the optimum concentration. Increase in concentration, increases the effective surface coverage and therefore increases  $\eta\%$ . On the basis of increase in inhibition efficiency with increasing INH concentration, it can be concluded that surface coverage and therefore inhibition efficiency increase with increasing inhibitor concentration. However, probably the maximum surface coverage was obtained at 50 mg/L concentration. Therefore, further increase in the concentration did not cause any significant increase in the surface coverage and inhibition efficiency by inhibitor.

### 3.1.2. Effect of temperature

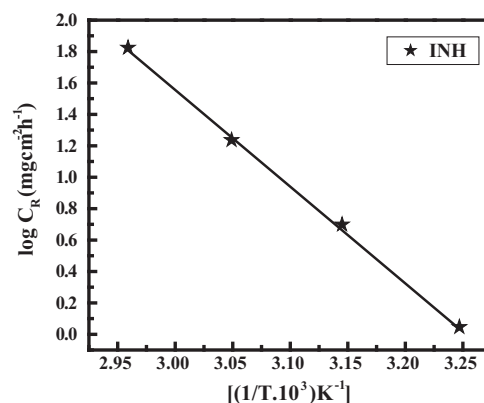
Effect of solution temperature on corrosion inhibition efficiency of INH in 1M HCl is shown in Fig. 2b. It is observed that the value of  $\eta\%$  decreases on increasing solution temperature. The increase in solution temperature increases the kinetic energy of the INH and therefore decreases the interaction between inhibitor and metal surface and thus decreases the inhibition efficiency [10]. Further, increases in the solution temperature cause molecular decomposition resulting into decrease in the inhibition efficiency. The effect of temperature on the nature of mild steel dissolution in 1M HCl can be best explained in terms of Arrhenius equation [11]:

$$\log(C_R) = \frac{-E_a}{2.303RT} + \log \lambda \quad (5)$$

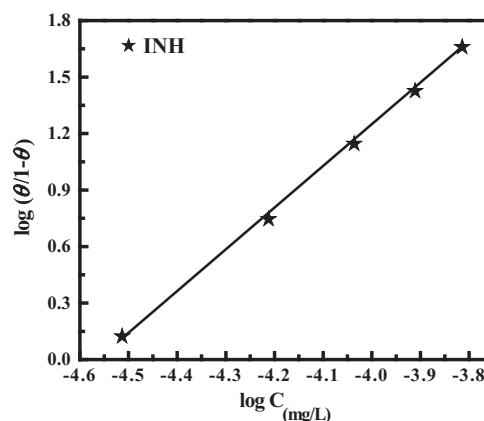
where  $C_R$  is the corrosion rate in mg cm<sup>-2</sup> h<sup>-1</sup>,  $\lambda$  is the Arrhenius pre-exponential factor,  $R$  is the gas constant and  $T$  is the absolute temperature. The values of  $E_a$  with and without INH were calculated with the help of slopes and intercepts of the Arrhenius plots (Fig. 3) and are given in Table 2. From the results depicted in Table 2 it is observed that the value of  $E_a$  is higher (117.11 kJ/mol) in presence of INH as compared to value of  $E_a$  in the absence of INH (28.48 kJ/mol), suggesting that INH inhibits mild steel corrosion by forming an energy barrier for corrosion process [12]. Moreover, electrostatic interaction (physical adsorption) between charged inhibitor and charged metal surface might cause this increase in the value of  $E_a$  in the presence of INH [13].

### 3.1.3. Adsorption isotherm

The mechanism of corrosion inhibition in acid solution as well as basic interaction between metal and inhibitor can be explained in terms of molecular adsorption. The adsorption of inhibitor on metal surface creates a barrier between metal and electrolyte which isolate the metal from aggressive

**Figure 3** Arrhenius plots for the corrosion rate of mild steel versus the temperature in 1M HCl.**Table 2** Values of activation energies for mild steel dissolution in 1M HCl in the absence and presence of INH.

Inhibitor	$\Delta E$
Blank	28.48
INH	117.11

**Figure 4** Langmuir isotherm plots for the adsorption of INH on mild steel surface in 1M HCl.

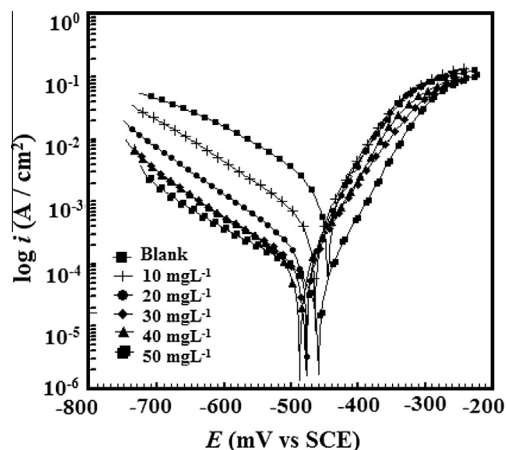
solution and protect from corrosion. In our present study several adsorption isotherms namely, Langmuir, Temkin, and Frumkin isotherms were tested to find best fit. The results showed that Langmuir isotherm gives the best fit with value of regression coefficient more close to unity ( $R^2 = 0.9999$ ). The Langmuir isotherms can be best represented by the following relation [14]:

$$K_{ads}C = \frac{\theta}{1 - \theta} \quad (6)$$

where  $C_{inh}$  is the concentration of inhibitor,  $\theta$  is the degree of surface coverage at different concentrations of the INH and  $K_{ads}$  is the equilibrium constant for adsorption-desorption process. The Langmuir isotherm plot (Fig. 4) gives a straight line between  $\log(\theta/1 - \theta)$  and  $\log C_{(mol/L)}$  for studied INH

**Table 3** The values of  $K_{\text{ads}}$  and  $\Delta G_{\text{ads}}^0$  for mild steel in 1M HCl at different studied temperature.

Inhibitor	$K_{\text{ads}}$ ( $10^4 \text{ M}^{-1}$ )				$-\Delta G_{\text{ads}}^0$ (kJ mol $^{-1}$ )			
	308	318	328	338	308	318	328	338
INH	9.043	1.157	0.603	0.365	39.52	35.36	34.70	34.34

**Figure 5** Polarization curves for mild steel in the absence and presence of different concentrations of INH.

with value of regression coefficient close to unity. The value of  $K_{\text{ads}}$  related to the free energy of adsorption  $\Delta(G_{\text{ads}}^0)$  is as follows:

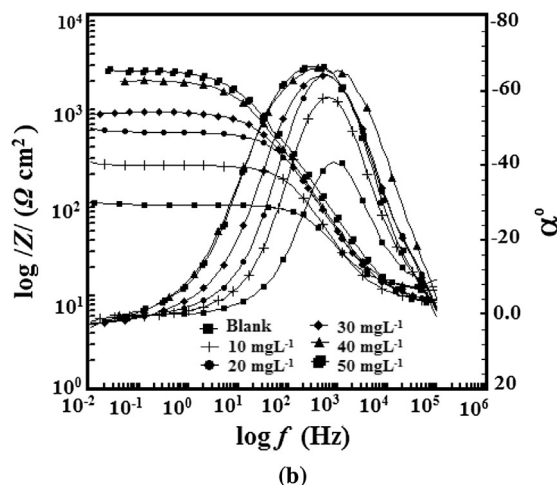
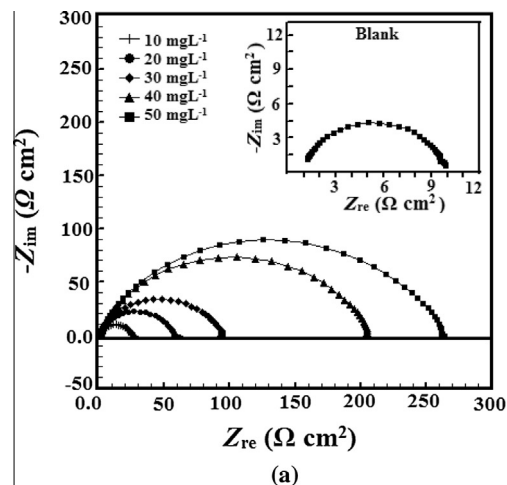
$$\Delta G_{\text{ads}}^0 = -RT \ln (55.5 K_{\text{ads}}) \quad (7)$$

where  $R$  is the universal gas constant,  $T$  is the absolute temperature in  $K$ , and the numerical value 55.5 represents the molar concentration of water in acid solution. The calculated values of  $K_{\text{ads}}$  and  $\Delta G_{\text{ads}}^0$  are given in Table 3. Generally, the higher value of  $K_{\text{ads}}$  was associated with strong adsorption and therefore, higher  $\eta\%$ . From Table 3 it is observed that values of  $\Delta G_{\text{ads}}^0$  range between 39.52 kJ/mol and 34.34 kJ/mol. The negative values of  $\Delta G_{\text{ads}}^0$  suggest that process of INH adsorption at mild steel surface in 1M HCl is spontaneous and mostly involves both physical and chemical interactions [15].

### 3.2. Electrochemical measurements

#### 3.2.1. Potentiodynamic polarization measurements

The potentiodynamic nature of mild steel in 1M HCl in the absence and presence of various concentrations of INH is shown in Fig. 5. Several polarization parameters such as

**Figure 6** (a) Nyquist plot for mild steel in 1M HCl without and with different concentrations of INH. (b) Bode ( $\log f$  vs  $\log |Z|$ ) and phase angle ( $\log f$  vs  $\alpha^\circ$ ) plots for mild steel in 1M HCl in the absence and presence of different concentration of INH.

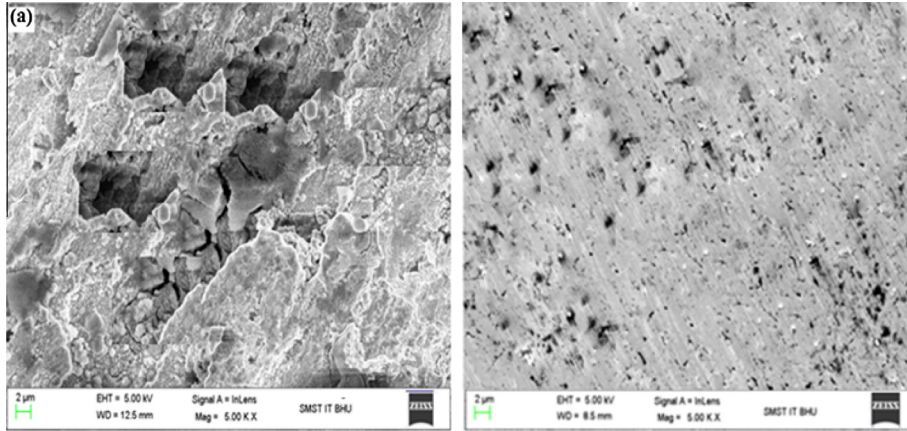
corrosion potential ( $E_{\text{corr}}$ ), corrosion current density ( $i_{\text{corr}}$ ), anodic and cathodic Tafel slopes ( $\beta_a$  and  $\beta_c$ ), surface coverage

**Table 4** Tafel polarization parameters for mild steel in 1M HCl solution in the absence and at different concentrations of INH.

Inhibitor	Conc (mg/L)	$E_{\text{corr}}$ (mV/SCE)	$i_{\text{corr}}$ ( $\mu\text{A}/\text{cm}^2$ )	$\beta_a$ (mV/dec)	$\beta_c$ (mV/dec)	$\theta$	$\eta\%$
Blank	–	–445	1150	70.5	114.6	–	–
INH	10	–465	462.3	61.2	130.3	0.5980	59.80
	20	–477	174.2	56.8	134.4	0.8485	84.85
	30	–479	119.3	63.6	189.0	0.8962	89.62
	40	–487	63.2	63.3	132.7	0.9449	94.49
	50	–459	42.6	60.3	185.7	0.9629	96.29

**Table 5** EIS parameters obtained for mild steel in 1M HCl without and with different concentration of INH.

Inhibitor	Conc (mg/L)	$R_s$ ( $\Omega$ cm <sup>2</sup> )	$R_{ct}$ ( $\Omega$ cm <sup>2</sup> )	$C_{dl}$ ( $\mu$ F cm <sup>-2</sup> )	$n$	$\theta$	$\eta\%$
Blank	–	1.12	9.58	106.21	0.827	–	–
INH	10	0.894	24.6	84.21	0.825	0.6105	61.05
	20	0.932	56.9	67.78	0.830	0.8316	83.16
	30	0.901	91.8	64.09	0.852	0.8956	89.56
	40	1.110	197.5	60.30	0.861	0.9514	95.14
	50	0.760	259.8	55.22	0.899	0.9631	96.31

**Figure 7** SEM images of mild steel (a) in blank acid solution and in the presence of 50 mg/L of (b) INH.

( $\theta$ ) and corresponding inhibition efficiency ( $\eta\%$ ) were calculated by extrapolation of linear segments of anodic and cathodic Tafel slopes and are given in Table 4. From the results shown in Table, it is observed that the presence of INH in acid solution affects the anodic rate of mild steel dissolution as well as rate of cathodic hydrogen evolution without causing any substantial decrease in the value of  $E_{corr}$  suggesting that INH is a mixed type inhibitor [16,17]. Further, results showed that the presence of INH decreases the values of corrosion current density ( $i_{corr}$ ) suggesting that rate of mild steel dissolution decreased in the presence of INH at various concentrations [18]. Further, decrease in  $i_{corr}$  values is more pronounced at higher INH concentration.

### 3.2.2. Electrochemical impedance spectroscopy

The electrochemical impedance spectroscopy is the most important electrochemical technique to study the kinetics and some structural properties of electric double layer. Fig. 6a shows the Nyquist plots for mild steel dissolution in the absence and presence of different concentrations of the INH. It is observed that diameter of the Nyquist plots increases with increasing INH concentration. Further, the Nyquist plots represent the imperfect semicircle which is attributed due to rough electrode surface and surface inhomogeneity. Several EIS parameters such as solution resistance ( $R_s$ ), charge transfer resistance ( $R_{ct}$ ), double layer capacitance ( $C_{dl}$ ), phase shift ( $n$ ), surface coverage ( $\theta$ ) and corresponding inhibition efficiency ( $\eta\%$ ) were calculated using an equivalent circuit described elsewhere [19] and are given in Table 5. From the EIS depicted in Table 5 it is observed that values of  $R_{ct}$  increase whereas the values of  $C_{dl}$  decrease in the presence of

INH at different concentration. This increase in  $R_{ct}$  and decrease in  $C_{dl}$  values in the presence of INH are attributed due to a decrease in local dielectric constant and/or to an increase in the thickness of the electrical double layer [20]. These results suggest that the studied INH inhibits mild steel corrosion by adsorbing at the metal/electrolyte interfaces.

The Bode plot (Fig. 6b) in the absence and presence of each studied concentration gives one time constant (single maximum) at intermediate frequencies. Broadening of the maximum is attributed due to adsorption of the INH at metal/electrolyte interface [19]. In the present investigation a linear relationship between  $\log |Z|$  and  $\log f$  with slope value close to  $-1$  and phase angle value close to  $-70^\circ$  was observed in the Bode plots. An ideal capacitor is characterized by a constant value of phase angle and slope equal to  $-90^\circ$  and  $-1$ , respectively. The deviation from the ideal capacitive behavior in present study is attributed due to roughness of the mild steel surface [20]. The careful observation of the Bode plots shows that values of phase angle are higher for inhibited solution as compared to uninhibited solution. Moreover, it can be further observed that the values of phase angle for inhibited solution increase on increasing INH concentration. The increased values of phase angle in the presence of INH suggest that mild steel surface smoothness increased due to formation of protective surface film by INH [20,21].

### 3.3. Surface measurements

#### 3.3.1. Scanning electron microscopy (SEM) study

The scanning electron microscopy (SEM) images of mild steel surface in the absence and presence of optimum concentration

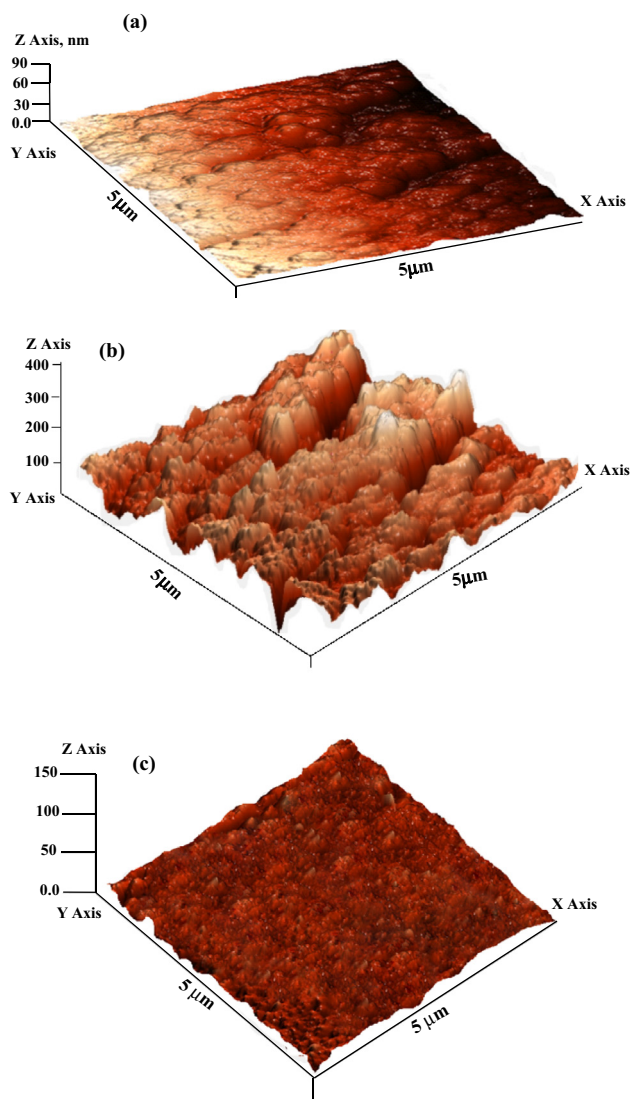


**Figure 8** The AFM micrographs of mild steel surface (a) abraded mild steel, (b) in blank acid solution and (c) in presence of INH.

of the investigated INH are shown in Fig. 7. The SEM image of mild steel in the absence of INH (Fig. 7a) was highly corroded and damaged which might be attributed to the free acid corrosion of the surface in the absence of INH. However, in the presence of INH at its optimum concentration (Fig. 7b) the surface morphology remarkable smoothed owing to the formation of protective surface film by INH.

### 3.3.2. Atomic force microscopy (AFM) study

The atomic force microscopy (AFM) micrographs for abraded, uninhibited and inhibited mild steel specimens are

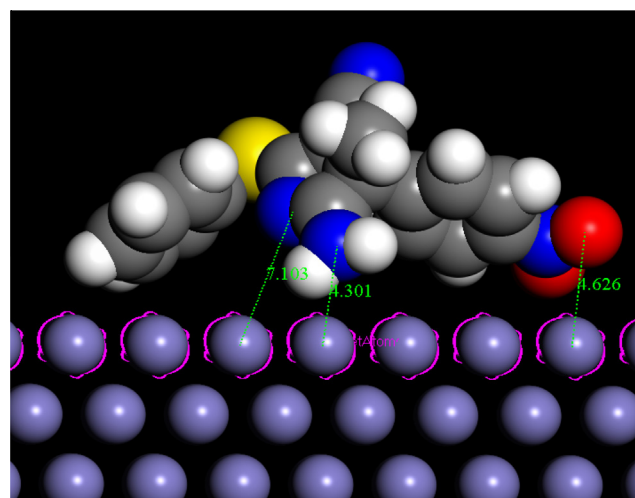


**Figure 9** The most stable low energy configuration for the adsorption of INH on Fe (110) surface obtained through the Monte Carlo simulations.

shown in Fig. 8. Fig 8a represents the AFM micrographs of abraded mild steel surface characterized by clear appearance of bradding scratches on the surface resulted due to mechanical rubbing with SiC emery paper during cleaning process. The calculated surface roughness of abraded mild steel specimens was 85 nm. The AFM micrograph for uninhibited solution (Fig. 8b) was highly corroded with characteristic pits and cracks. The calculated surface roughness for uninhibited mild steel specimen was 392 nm. The higher surface roughness is attributed due to free acid corrosion of mild steel in the absence of INH. However, in the presence of INH at its optimum concentration the surface smoothness increases due to formation of protective surface film. In the presence of INH the average surface roughness of mild steel was 146 nm. The decrease in the surface roughness in the presence of INH (146 nm) than in absence of INH (392 nm) suggests that in the presence of INH surface of mild steel is less corroded and damaged due to formation of protective film by INH. However, the surface roughness is comparatively high in the presence of INH as compared to abraded mild steel surface which is attributed to some extent of corrosion even in the presence of INH.

### 3.4. Monte Carlo simulation

Recently, molecular dynamics simulation has been broadly used to describe the interaction between metal and inhibitor because it provides some essential parameters such as total energy, adsorption energy, and rigid adsorption energy. In our present study, the Monte Carlo simulation calculation was used to find the lowest energy for the investigated system. The outputs and descriptors calculated by the Monte Carlo

**Table 6** Outputs and descriptors calculated by the Monte Carlo simulation for the lowest adsorption configurations of INH on Fe (110) surface (in kcal/mol).

Systems	Total energy	Adsorption energy	Rigid adsorption energy	Deformation energy	$dE_{ad}/dN_i$ Inhibitors
Fe (110)/INH	56.486	-4.051	-4.196	0.014	-4.051

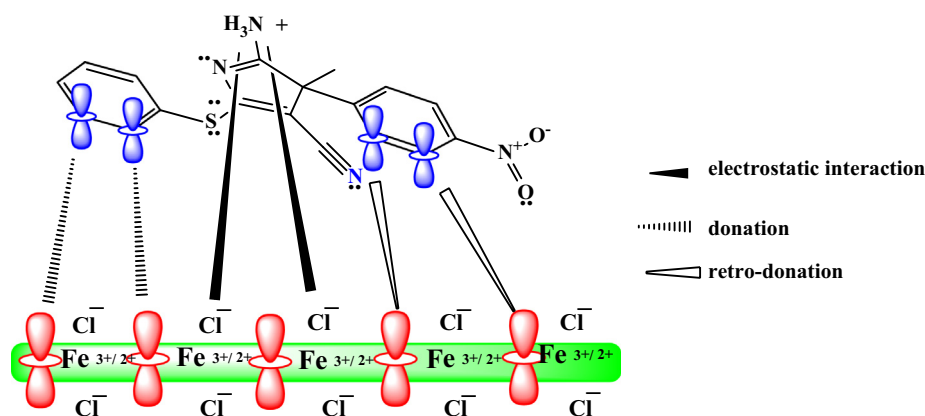


**Figure 10** Pictorial representation of the adsorption behavior of the INH on mild steel in 1M HCl solution.

simulation, such as the total adsorption, adsorption energy, rigid adsorption and deformation energies are presented in Table 6. Fig. 9 represents the most stable low energy configuration for the adsorption of INH on Fe (110) surface obtained through the Monte Carlo simulations. The sum of rigid adsorption energy and deformation energy is defined as adsorption energy for the adsorbate component (INH), whereas, the rigid adsorption energy is the energy in kcal/mol which is either released or absorbed when the unrelaxed INH molecule was adsorbed on the  $\text{Fe}_2\text{O}_3$  surface. The deformation energy is the energy (in kcal/mol) released when the adsorbed adsorbate components are relaxed on the  $\text{Fe}_2\text{O}_3$  surface [22]. The quantity  $(dE_{\text{ads}}/dN_i)$  depicted in Table 6 represents the energy of  $\text{Fe}_2\text{O}_3$ -adsorbate configurations where one of the adsorbate components has been removed. The results depicted in Table 6 show that the INH was associated with high negative values of adsorption energy resulting in the strong interaction between metal and INH molecule [21].

#### 4. Mechanism of inhibition

The mechanism of mild steel corrosion in the presence of 2-amino-3-methyl-3-(4-nitrophenyl)-5-(phenylthio)-3H-pyrrole-4-carbonitrile can be explained on the basis of molecular adsorption. The adsorption of organic inhibitor on metal surface may be either pure physical or pure chemical or the combination of both i.e. physiochemisorption [23]. Generally, physical adsorption involves electrostatic interaction between charged metal and charged inhibitor molecule whereas chemisorption involves sharing of charges between metal and inhibitor. It has been established that in acid solution heteroatoms (N, O, S, etc.) undergo easy protonation to give positively charged inhibitor. This positively charged inhibitor electrostatically interacts with negative charged mild steel surface (due to presence of surface chloride ions). However, after evolution of  $\text{H}_2$  gas at cathode the cationic form of inhibitor returns to its neutral form. The neutral form of inhibitor adsorbs chemically by transfer of unshared paired electrons of heteroatoms in the d-orbital of the surface Fe-atoms (donation). However, this type of donation causes accumulation of excessive charges on the metal surface and to relief from excessive charges the transfer of electrons from d-orbital of the surface Fe-atoms in the  $\pi$ -antibonding molecular orbitals of the inhibitor takes place (retro-donation). This type donation and retro-

donation strengthen each other through synergism [24,25]. The higher inhibition efficiency of the investigated INH can be explained on the basis of strong interaction between metal and INH through several polar groups (such as  $-\text{NO}_2$ ,  $-\text{NH}_2$ ,  $-\text{CN}$ ), heteroatoms (N, O, S), and aromatic as well as hetero-aromatic rings. Further, the presence of polar functional groups and heteroatoms also increases the solubility of the INH in 1M HCl and therefore increases the inhibition efficiency [26]. A pictorial representation of the adsorption behavior of the INH on mild steel in 1M HCl solution is shown in Fig. 10.

#### 5. Conclusion

From the above study it is concluded that 2-amino-3-methyl-3-(4-nitrophenyl)-5-(phenylthio)-3H-pyrrole-4-carbonitrile (INH) exhibited good inhibition efficiency on mild steel in 1M HCl. The inhibition efficiency increases on increasing INH concentration and maximum value was obtained at 50 mg/L concentration. The adsorption of INH on mild steel surface obeys the Langmuir adsorption isotherm. Potentiodynamic polarization study shows that studied INH is a mixed type inhibitor. EIS study shows that the INH forms a protective surface film on metal/electrolyte interface. The formation of protective surface film was further supported by SEM and AFM analysis. The molecular dynamics simulations study supports the weight loss, electrochemical and surface measurements and established that there is strong interaction between mild steel and the INH.

#### Acknowledgment

Chandra Bhan Verma gratefully acknowledges Ministry of Human Resource Development (MHRD), New Delhi (India), for providing financial assistance and facilitation for present study.

#### References

- [1] Yildiz R. An electrochemical and theoretical evaluation of 4,6-diamino-2-pyrimidinethiol as a corrosion inhibitor for mild steel in HCl solutions. *Corros Sci* 2015;90:544–53.
- [2] Ji G, Shukla SK, Dwivedi P, Sundaram S, Prakash R. Inhibitive effect of Argemone mexicana plant extract on acid corrosion of mild steel. *Ind Eng Chem Res* 2011;50:11954–9.



- [3] Caliskan N, Akbas E. The inhibition effect of some pyrimidine derivatives on austenitic stainless steel in acidic media. *Mater Chem Phys* 2011;126:983–8.
- [4] Yadav M, Behera D, Kumar S, Sinha RR. Experimental and quantum chemical studies on the corrosion inhibition performance of benzimidazole derivatives for mild steel in HCl. *Ind Eng Chem Res* 2013;52:6318–28.
- [5] Hegazy MA, Abdallah M, Awad MK, Rezk M. Three novel diquaternary ammonium salts as corrosion inhibitors for API X65 steel pipeline in acidic solution. Part I: Experimental results. *Corros Sci* 2014;81:54–64.
- [6] Tang Y, Yang X, Yang W, Chen Y, Wan R. Experimental and molecular dynamics studies on corrosion inhibition of mild steel by 2-amino-5-phenyl-1,3,4-thiadiazole. *Corros Sci* 2010;52:242–9.
- [7] Das P, Ray S, Mukhopadhyay C. Exploitation of dual character of CN moiety in the synthesis of uniquely decorated 3H-pyrroles: a rare observation. *J Org Lett* 2015;15:5622–5.
- [8] Verma CB, Quraishi MA, Ebenso EE. Electrochemical studies of 2-amino-1, 9-dihydro-9-((2-hydroxyethoxy) methyl)-6H-purin-6-one as green corrosion inhibitor for mild steel in 1.0 M hydrochloric acid solution. *Int J Electrochem Sci* 2013;8:7401–13.
- [9] Obot IB, Umoren SA, Gasem ZM, Suleiman R, El Ali B. Theoretical prediction and electrochemical evaluation of vinylimidazole and allylimidazole as possible green corrosion inhibitors for carbon steel in 1M HCl. *J Ind Eng Chem* 2015;21:1328–39.
- [10] Alijourani J, Raeissi K, Golozar MA. Benzimidazole and its derivatives as corrosion inhibitors for mild steel in 1M HCl solution. *Corros Sci* 2009;51:1836–43.
- [11] Mahmoud MA. Kinetics and thermodynamics of aluminum oxide nanopowder as adsorbent for Fe (III) from aqueous solution. (*BJBAS*) Beni-Suef Univ J Basic Appl Sci 2015;xxx:1–8. <http://dx.doi.org/10.1016/j.bjbas.2015.05.008>.
- [12] Verma CB, Singh A, Pallikonda G, Chakravarty M, Quraishi MA, Bahadur I, Ebenso EE. Aryl sulfonamidomethylphosphonates as new class of green corrosion inhibitors for mild steel in 1M HCl: electrochemical, surface and quantum chemical investigation. *J Mol Liq* 2015;209:306–19.
- [13] Verma C, Quraishia MA, Olasunkanmi LO, Ebenso EE. L-proline-promoted synthesis of 2-amino-4-arylquinoline-3-carbonitriles as sustainable corrosion inhibitors for mild steel in 1M HCl: experimental and computation studies. *RSC Adv* 2015. <http://dx.doi.org/10.1039/C5RA16982H>.
- [14] Verma CB, Quraishi MA, Ebenso EE. Electrochemical and thermodynamic investigation of some soluble terpolymers as effective corrosion inhibitors for mild steel in 1M hydrochloric acid solution. *Int J Electrochem Sci* 2013;8:12894–906.
- [15] Yıldız R, Dogan T, Dehri I. Evaluation of corrosion inhibition of mild steel in 0.1M HCl by 4-amino-3-hydroxynaphthalene-1-sulphonic acid. *Corros Sci* 2014;85:215–21.
- [16] Barmatov E, Hughes T, Nagl M. Experimental and theoretical study on corrosion inhibition of oxime compounds for aluminium in HCl solution. *Corros Sci* 2014;81:162–75.
- [17] Khaled KF, Amin MA. Corrosion monitoring of mild steel in sulphuric acid solutions in presence of some thiazole derivatives – molecular dynamics, chemical and electrochemical studies. *Corros Sci* 2009;51:1964–75.
- [18] Anejjar A, Salghi R, Zarrouk A, Benali O, Zarrok H, Hammouti B, Ebenso EE. Inhibition of carbon steel corrosion in 1M HCl medium by potassium thiocyanate. *J Asso Arab Univ Basic App Sci* 2014;15:21–7.
- [19] Verma CB, Reddy MJ, Quraishi MA. Microwave assisted eco-friendly synthesis of chalcones using 2, 4-dihydroxy acetophenone and aldehydes as corrosion inhibitors for mild steel in 1M HCl. *Anal Bioanal Electrochem* 2014;6:321–40.
- [20] Verma CB, Singh P, Bahadur I, Ebenso EE, Quraishi MA. Electrochemical, thermodynamic, surface and theoretical investigation of 2-aminobenzene 1,3-dicarbonitriles as green corrosion inhibitors for aluminum in 0.5 M NaOH. *J Mol Liq* 2015;209:767–78.
- [21] Khaled KF, Amin MA. Dry and wet lab studies for some benzotriazole derivatives as possible corrosion inhibitors for copper in 1.0 M HNO<sub>3</sub>. *Corros Sci* 2009;51:2098–106.
- [22] Guo L, Zhu S, Zhang S, He Q, Li W. Theoretical studies of three triazole derivatives as corrosion inhibitors for mild steel in acidic medium. *Corros Sci* 2014;87:366–75.
- [23] Ahamad I, Prasad R, Quraishi MA. Adsorption and inhibitive properties of some new Mannich bases of Isatin derivatives on corrosion of mild steel in acidic media. *Corros Sci* 2010;52(2):1472–81.
- [24] Yadav DK, Maiti B, Quraishi MA. Electrochemical and quantum chemical studies of 3,4-dihydropyrimidin-2(1H)-ones as corrosion inhibitors for mild steel in hydrochloric acid solution. *Corros Sci* 2010;52:3586–98.
- [25] Verma CB, Singh P, Quraishi MA. A thermodynamical electrochemical and surface investigation of Bis (indolyl) methanes as Green corrosion inhibitors for mild steel in 1M hydrochloric acid solution. *J Asso Arab Univ Basic App Sci* 2015. <http://dx.doi.org/10.1016/j.jaubas.2015.04.003>, xx:.
- [26] Verma CB, Singh P, Quraishi MA, Singh A. A thermodynamical, electrochemical, theoretical and surface investigation of diheteroaryl thioethers as effective corrosion inhibitors for mild steel in 1M HCl. *J Taiwan Inst Chem Eng* 2015. <http://dx.doi.org/10.1016/j.jtice.2015.06.020>.



**Mr. Chandrabhan Verma** is research Scholar in Department of chemistry, IIT (BHU), Varanasi (India). He obtained B.Sc. (2007) and M.Sc. (2010) degrees from Purvanchal University (UP College). Also, He has published several research papers in the referred international journals in the field of corrosion.



**M.A. Quraishi** is professor in Department of chemistry, IIT (BHU), Varanasi (India). He received B.Sc. (1969) degree and M.Sc. (1971) degree from Saugar University, M. Phil (1978) and Ph. D (1986) from Kurukshetra University, and D.Sc. (2004) from centrally funded AMU Aligarh. Before joining as Professor at BHU, he was Reader (1990–2005) at AMU Aligarh. He has published a number of papers in different reputed journals. Also, he has published several research papers in the

referred international journals and many papers in national/international conferences.